Research Square

Preprints are preliminary reports that have not undergone peer review.
They should not be considered conclusive, used to inform clinical practice,
or referenced by the media as validated information.

Machine learning algorithms for plasma AD biomarkers implementation in two real-world cohorts

Edoardo Guido Torrigiani
University of Perugia
Giovanni Bellomo
Link Campus University
Davide Cianca
University of Perugia
Giovanna Nardi
University of Perugia
Igor Neri
University of Perugia
Davide Chiasserini
University of Perugia
Luisa Agnello
University of Palermo
Marcello Ciaccio
University of Palermo
Tommaso Piccoli
University of Palermo
Lucilla Parnetti
University of Perugia
Lorenzo Gaetani
lorenzo.gaetani@unipg.it
University of Perugia
Luca Gammaitoni
University of Perugia

Research Article

Keywords: Alzheimer’s disease, plasma, biomarkers, machine learning, p-Tau181, p-Tau217, cut-offs

Posted Date: March 12th, 2026

DOI: https://doi.org/10.21203/rs.3.rs-8987177/v1

License: This work is licensed under a Creative Commons Attribution 4.0 International License. Read Full License

Additional Declarations: Competing interest reported. G. Bellomo received honoraria from Fujirebio and completed paid consultancies for Parkinson’s Foundation. He received travel/educational grants from Fujirebio and Alzheimer’s Association. L. Parnetti served as Member of Advisory Boards for Fujirebio, IBL, Roche, and Merck. L. Gaetani has participated in advisory boards for and received writing or speaker honoraria and travel grants from Biogen, Eisai, Euroimmun, Fujirebio, Lilly, Novartis, Roche, and Siemens Healthineers. M. Ciaccio served as Member of Advisory Boards for Roche, Novartis and Lilly. L. Agnello served as Member of Advisory Boards for Novartis and Lilly. E.G. Torrigiani, D. Cianca, G. Nardi, I. Neri, L. Gammaitoni and D. Chiasserini have nothing to disclose.

Abstract

Background.

Blood-based biomarkers (BBMs) have shown high accuracy for Alzheimer's Disease (AD) diagnosis in highly selected cohorts. In view of the introduction of plasma biomarkers in larger cohorts in real-world clinical settings, we wanted to assess whether machine learning (ML) approaches could generate reliable cutoffs for BBMs, independently from the availability of CSF or Aβ-PET gold standard reference.

Methods.

Supervised and unsupervised ML models were applied to combined plasma pTau181 and Aβ42/40 and to plasma pTau217 alone for AD classification in a real-world cohort from Perugia University Hospital (UniPg cohort), including patients with AD (n = 285), patients with other neurodegenerative disorders (n = 144) and neurological controls (n = 172) for which paired CSF AD-biomarkers were available. Cutoffs obtained for plasma pTau217 were also tested in an independent cohort from Palermo University Hospital (UniPa cohort), which included CSF confirmed AD (n = 89) and non-AD patients (n = 29).

Results.

Cutoffs obtained from unsupervised GMM clustering achieved a comparable diagnostic accuracy with respect to traditional CSF-based ROC analysis both for plasma pTau181 (~ 78%) and Aβ42/40 (~ 76%) combined and for plasma pTau217 alone (~ 86%) in UniPg cohort. The combined use of clustering-obtained cutoffs for plasma pTau181 and Aβ42/40 reached an accuracy comparable to the one of pTau217 alone for AD diagnosis in UniPg cohort. Supervised ML models for AD classification (Support Vector Machines and XGBoost) did not outperform unsupervised GMM clustering in UniPg cohort. CSF and clustering-based cutoffs for plasma pTau217 in UniPg cohort reached a comparable accuracy also when applied to UniPa independent cohort (~ 85%).

Conclusions.

Our unsupervised clustering algorithm enables the definition of reliable cutoffs for blood-based AD biomarkers independently from CSF data in a large, heterogeneous real-world cohort. Cutoffs obtained from unsupervised clustering in UniPg cohort showed a comparable accuracy when applied to an independent validation cohort (~ 85% in UniPa cohort). In UniPg cohort, the combined use of plasma pTau181 and Aβ42/40 increased their diagnostic accuracy, supporting the utility of multiple BBMs testing.

Background

Blood-based biomarkers (BBMs) have shown great potential as a scalable, minimally invasive tool for Alzheimer's Disease (AD) diagnosis [1–3]. The availability of fully automated techniques[4–6] has made it possible to reliably measure biomarkers of AD in plasma. Among AD BBMs, pTau isoforms, particularly pTau217[7–10], have shown the highest diagnostic accuracy in differentiating AD from control subjects [11,12]. These advancements have recently led to the inclusion of BBMs among core biomarkers of AD[13] and to their recent approval as diagnostic tools for AD by FDA[14].

BBMs diagnostic accuracy for AD has been proved in selected cohorts (i.e., AD vs. controls) and reliable cohort-specific cutoff values have been defined with respect to CSF or amyloid PET positivity. In real-world settings, additional evidence is required regarding the possibility to establish reliable cutoffs for plasma biomarkers without gold standard reference biomarkers.

To this point, unsupervised clustering [15] may be used to define cutoffs for AD BBMs independently from the availability of CSF or nuclear imaging data. Applying unsupervised Gaussian mixture model (GMM) clustering to CSF AD biomarkers has already led to derive cutoffs independently from neuropathological evidence [16].

In this study, a GMM clustering approach has been applied to establish cutoff values for two model BBMs (plasma Aβ42/40 and pTau181) and for pTau217, the most promising standalone BBM of AD, in a real-world cohort from Perugia University Hospital (UniPg cohort) for which paired CSF A/T/(N) profiles were available. The performances of this unsupervised CSF-independent approach for cutoff definition of AD BBMs have been compared to classical CSF-based ROC analysis and state-of-art supervised machine learning (ML) algorithms in UniPg cohort and tested in an independent external validation cohort from Palermo University Hospital (UniPa cohort), for which paired CSF biomarkers profile and plasma pTau217 were available.

Methods

Participants

We selected a retrospective cohort of 601 consecutive patients who referred to the Neurology Clinic of the University Hospital of Perugia (UniPg cohort) and a retrospective consecutive cohort of 118 consecutive patients from the Neurology Clinic of the University Hospital of Palermo (UniPa cohort) (**Table 1**). All subjects underwent a thorough diagnostic workup, including medical history assessment, clinical examination, neuropsychological evaluation (at least comprehensive of Mini-Mental State Examination[17] and Clinical Dementia Rating scale [18]), brain MRI scan, laboratory tests, lumbar puncture and blood sampling. Diagnosis was based on the complete clinical-biological profile of each patient, according to diagnostic criteria, for each condition (Alzheimer's Disease in all its clinical stages, Parkinson's disease both with and without cognitive impairment, Parkinson's disease dementia/dementia with Lewy Bodies, Fronto-temporal dementia)[19 20 21 22 23 24]. Patients with subjective cognitive complaints or other neurological conditions (headache, mood disorders, vascular white matter lesions) and with a non-AD CSF A/T/(N) biomarker profile were included as control subjects (CTRL).

Biomarker measurements

CSF was collected and analyzed according to international guidelines[25]. Measures were performed with the fully automated chemiluminescent platform Lumipulse G600-II or Lumipulse G1200 (Fujirebio Inc) for β-amyloid 1-42 (Aβ42), β-amyloid 1-40 (Aβ40), tTau and pTau181 levels, according to the instructions from the manufacturer. CSF A/T/(N) profiles were evaluated according to previously published cutoffs[16] for both UniPg and UniPa cohorts.

Plasma Aβ40, Aβ42, pTau181 and pTau217 measurements were performed on the Lumipulse G1200 according to the instructions from the manufacturer. In UniPg cohort, plasma Aβ40, Aβ42, and pTau181 were measured for all patients, while plasma pTau217 was measured for a subgroup of 490 patients (preAD=24, AD-MCI=127, AD-dem=95, FTD=18, OND=32, PD-CN=36, PD-MCI=43, PDD/DLB=11, CTRL=104) in the UniPg Cohort. For the UniPa cohort, plasma pTau217 was available for all 118 patients (**Table 1**).

All measurements for UniPg cohorts were performed at the Laboratory of Clinical Neurochemistry, Section of Neurology, Department of Medicine and Surgery, University of Perugia, Perugia (IT) while for UniPa cohort the measurements were performed at Institute of Clinical Biochemistry, Clinical Molecular Medicine, and Clinical Laboratory Medicine, Department of Biomedicine, Neurosciences and Advanced Diagnostics, University of Palermo, Palermo (IT).

Data analysis

A first, unrestrained clustering algorithm based on Gaussian Mixture Model (GMM) was applied to generate clusters based on Aβ42/40 and pTau181 distribution in UniPg cohort. The optimal number of clusters was obtained by minimizing Bayesian Information Criterion (BIC) [26]. Clusters obtained were labeled as AD and non-AD according to the prevalence of clinical suspect of AD at first clinical evaluation; the prevalence of an A+/T+ CSF profile in each cluster was then evaluated (**Supplementary Figure 1**).

After removing outliers via inter-quartile range (IQR) criterion, the GMM clustering algorithm was applied to plasma pTau181 and plasma Aβ42/40 distributions, forcing the number of clusters to two.

By analyzing the probability distribution of the gaussian model, a three-part cutoff [27,28] was defined (50% cluster 1, 95% cluster 1 and 5% cluster 1, respectively) for each BBM. The same three-part paradigm was applied to CSF-based (i.e., A+/T+ vs. non-A+/T+) ROC generated cutoffs for each biomarker. The accuracy of cutoff values generated via unsupervised clustering to predict an AD CSF profile was tested and confronted with the accuracy of the CSF-based ROC generated cutoffs.

A Support Vector Machine algorithm (SVM) [29] with Radial Basis Function (RBF) kernel and an XGBoost [30,31] algorithm with depth equal to 2.0 were applied to discriminate between AD and non-AD-labeled patients (according to CSF profile) based on plasma Aβ42/40 and pTau181. All accuracies obtained by unsupervised algorithms were verified by training and testing algorithms on whole UniPg database and by 10-fold cross-validation.

The same unsupervised paradigm was applied to the subset of patients in the UniPg cohort for which plasma pTau217 was available: after outlier removal via IQR criterion, cutoff values were generated both via CSF-reference (i.e., A+/T+ vs. non-A+/T+) and via unidimensional unsupervised GMM-clustering with cluster number forced to two.

Accuracies, sensitivities and specificities for AD diagnosis of cutoffs generated for plasma pTau217 in UniPg cohort were also measured in UniPa cohort (**Table 2 a and b**).

All cutoff accuracies, sensitivities and specificities were tested via 10-fold cross-validation.

All of the analyses were performed via Python v3.8 using matplotlib[32], scipy[33], seaborn[34], numpy[35], pandas [36], scikit-learn[37], scikit_posthocs[38], xgboost[30] libraries and R v4.2.1 packages [39].

Results

Study design

The design of the study is graphically summarized in **Figure 1**. Briefly, unsupervised GMM clustering, traditional CSF-based ROC analysis and supervised ML approaches were applied to the combination of plasma Aβ42/40 and pTau181 and to pTau217 alone from a real-world memory clinic cohort (UniPg cohort). In GMM clustering the cluster number was forced to two and a three-part cutoff was generated for each biomarker to distinguish between the two clusters. A three-part cutoff was also calculated via CSF-based ROC analysis for each BBM, while for supervised ML models a binary classification was obtained. The accuracies of these three approaches were compared by cross-validation in both cohorts.

Demographic and clinical details of the cohorts

Demographic and clinical characteristics of the cohorts are summarized in **Table 1**. Plasma biomarker concentrations, years of education and MMSE scores are presented as mean ± standard deviation. As expected, plasma biomarker concentrations, MMSE, and education differed among AD and non-AD groups ($p < 0.005$). Of interest, both pTau181 and pTau217 levels showed a significant progressive increase from preAD to ADdem in UniPg cohort. This trend was confirmed also in AD-MCI and ADdem patients in UniPa cohort, which did not include preAD patients.

Unrestrained clustering

The unrestrained GMM clustering algorithm spontaneously identified three clusters based on plasma Aβ42/40 and pTau181 distributions in UniPg cohort (**Supplementary Figure 1**). Clusters were then labeled, based on the initial clinical suspect, as AD (cluster 0, in which a 75% prevalence of AD clinical suspect was found), non-AD (cluster 1, with a 34% prevalence of AD clinical suspect) and undetermined (cluster 2, with an almost equal presence of AD and non-AD clinical suspect). The prevalence of CSF-confirmed AD diagnosis in each cluster was then evaluated. In Cluster 0, labeled as AD, the prevalence of CSF confirmed AD diagnosis was 87%. In Cluster 1, labeled as non-AD, the prevalence of a CSF confirmed diagnosis of AD was 15%. In Cluster 2, labeled as undetermined, the prevalence of a CSF confirmed diagnosis of AD was 58% (**Supplementary Table 1**).

Cutoff determination

All measured cutoffs for UniPg cohort are listed in **Table 2** and graphically presented in **Figure 2** and **Figure 3**. **Figure 4** shows the application to UniPa cohort of cutoffs derived in UniPg cohort for plasma pTau217.

After running the bidimensional GMM clustering algorithm with cluster number forced to two, a three-part cutoff was determined for Aβ42/40 ratio (best cutoff: 0.0817) and for plasma pTau181 (best cutoff: 2.15 pg/mL).

A CSF-based ROC analysis was performed to identify a cutoff value for plasma Aβ42/40 ratio (best cutoff: 0.0816) to predict a CSF A+ status, and for plasma pTau181 (best cutoff: 2.06 pg/mL) to predict a CSF A+T+ status.

Clustering-based and ROC-based cutoffs for 95% specificity and 95% sensitivity are listed in Tab. 2.

Then, the accuracy of each plasma pTau181 cutoff value to predict an A+/T+ CSF profile was tested. The accuracy of the best cutoff value (maximizing YI) generated via ROC analysis with CSF profile as a reference was 78.96%. The accuracy of the clustering-based cutoff was 78.6% (**Table 2**).

Similarly, the accuracy of each Aβ42/40 cutoff value to predict an A+ CSF profile was tested, with a value of 75.97% for the CSF-based cutoff. The accuracy of the clustering -based cutoff for plasma Aβ42/40 was 76.1% (**Table 2**).

We next explored the combined use of the cutoffs generated by clustering. for patients with both plasma Aβ42/40 lower than cutoff of 0.0817 and plasma pTau181 higher than cutoff of 2.15 pg/mL, the prevalence of a CSF confirmed AD profile was 87.3%. For patients with both plasma Aβ42/40 higher than cutoff of 0.0817 and plasma pTau181 lower than cutoff of 2.15 pg/mL, the prevalence of a CSF confirmed non-AD profile was 87.2%.

Unidimensional clustering for plasma pTau217 with cluster number forced to two led to the definition of two clusters in the UniPg cohort with a prevalence of an AD-CSF profile, respectively, of 14.1% in cluster 1 and 85% in cluster 2 (**Supplementary**

Table 1). According to unidimensional clustering distribution, a three-part cutoff was derived as above for UniPg cohort (best cutoff: 0.258 pg/mL).

The best cutoff generated via CSF-based ROC analysis for plasma pTau217 in UniPg cohort was 0.192 pg/mL. Clustering-based and ROC-based pTau217 cutoffs for 95% specificity and 95% sensitivity are listed in **Table 2**.

For the cutoff value generated analyzing plasma pTau217 clustering probability distribution, the accuracy in predicting an AD CSF profile was 86.1% while for the cutoff generated maximizing YI via CSF-based ROC analysis the accuracy in predicting an AD CSF profile was of 86.1% (**Table 2**, **Figure 3**).

Accuracies, sensitivities and specificities of UniPg generated cutoffs were tested for AD diagnosis in UniPa cohort and validated via 10-fold cross-validation.

Mean accuracies of the application to UniPa cohort of clustering-generated and CSF-ROC generated UniPg cutoffs were equivalent (85% for clustering-based cutoff vs. 84.2% for CSF-ROC based cutoff, respectively) (**Table 2 b, Figure 4**).

Supervised ML classification

State-of-art supervised ML classification algorithms were tested on plasma Aβ42/40 and pTau181 in UniPg cohort. The XGBoost algorithm, run with clinical and biological entry data (plasma Aβ42/40 and pTau181, age, education and MMSE at baseline evaluation) classified AD patients with an accuracy of 0.74 after training and testing on the whole database. Of interest, XGBoost classifier included, as significant variables, exclusively plasma pTau181 and plasma Aβ42/40. XGBoost results reached an equivalent accuracy when tested in a 10-fold cross-validation with 70-30% training-test set split.

Based on these findings a SVM model with RBF kernel was set to discriminate between CSF-defined AD and non-AD patients upon plasma pTau181 and plasma Aβ42/40 values in UniPg cohort. SVM-RBF reached an accuracy of 0.78 both when trained and tested in whole database and after 10-fold cross-validation with 70-30% training-test set split (**Figure 5**).

Discussion and limitations

Our results show that a CSF-independent pipeline based on GMM clustering followed by probability distribution analysis can achieve an accuracy equivalent to that obtained via CSF-based ROC analysis in cutoff definition for AD BBMs.

This finding is of great interest considering the heterogeneity of UniPg cohort, which included all clinical stages of AD, patients with co-morbidities that may alter plasma biomarker assessment (e.g. renal impairment, see **Supplementary Table 2**)[40], well-represented groups with unclear CSF profiles (A-/T+ n=54 and A+/T- n=53, see Tab. S2), as well as participants with neurodegenerative conditions other than AD and controls.

When the same analytical pipeline was applied to plasma pTau217, currently regarded as the most reliable standalone plasma biomarker of AD, the unsupervised approach defined a cutoff for AD classification independently of CSF profiling that achieved an accuracy equivalent to the CSF-based ROC model in the UniPg cohort. As expected, in UniPg cohort, plasma pTau217 alone outperformed pTau181 as a diagnostic biomarker of AD. Notably, the three-part cutoff generated via unsupervised clustering for pTau217 showed a narrower range with respect to the one generated via traditional CSF-based ROC analysis; a possible explanation for this result is that confounding factors (i.e. renal impairment) can elevate plasma pTau217 concentrations also in non-AD individuals, thus hampering the concordance between BBM- and CSF-based classification and leading to a wider range between 95% sensitivity and 95% specificity CSF-based cutoffs. The robustness of cutoffs defined in UniPg cohort for plasma pTau217 is reflected by the results obtained when the same cutoffs were applied to UniPa cohort.

Possible explanations for the slightly lower accuracies, sensitivities and specificities found in UniPa cohort can be the lower sample size and the larger prevalence of AD patients in this cohort (which included 89 AD patients and 29 non-AD patients) with only 10 non-AD patients having an A-/T- CSF profile (**Supplementary Table 2b**).

Of interest, by combining the two cutoffs identified through our unsupervised ML approach for plasma Aβ42/40 ratio and pTau181 in UniPg cohort, we achieved the best nominal concordance with CSF-confirmed diagnosis of AD (87.3%).

Furthermore, when applied to plasma Aβ42/40 ratio and pTau181, in UniPg cohort, state-of-art supervised classification algorithms did not outperform unsupervised GMM clustering-based classification.

Conclusions

Our findings address a key requirement for the real-world implementation of blood-based biomarkers for AD: establishing reliable diagnostic cutoffs when CSF or amyloid-PET data are not largely available. Our results demonstrate that an unsupervised machine-learning pipeline can define plasma-based cutoffs with accuracy equivalent to traditional CSF-guided approaches in a large, real-world cohort and that those cutoffs can be applied even to a smaller, imbalanced cohort with equivalent accuracy. Importantly, our unsupervised pipeline can be extended to any number of biomarkers. In the present study, we limited the analysis to either two markers, plasma Aβ42/40 and pTau181, or a single marker, pTau217, to facilitate intuitive interpretation and visualization and to evaluate the robustness of the methodology. As the combination of those two less reliable biomarkers outperformed a single-biomarker approach, an extension to broader biomarker panels could further improve diagnostic performance and strengthen the clinical value of BBMs in AD diagnosis.

Abbreviations

AD: Alzheimer's disease

ADdem: Alzheimer's disease dementia

AD-MCI: mild cognitive impairment due to Alzheimer's disease

BBM(s): blood-based biomarker(s)

BIC: Bayesian information criterion

CDR: clinical dementia rating scale

CSF: cerebro-spinal fluid

CTRL: control

DLB: dementia with Lewy bodies

FTD: fronto-temporal dementia

GMM: gaussian mixture model

IQR: inter-quartile range

MCI: mild cognitive impairment

ML: machine learning

MMSE: mini-mental state examination

MRI: magnetic resonance imaging

PD: Parkinson's disease

PD-MCI: Parkinson's disease with mild cognitive impairment

PDD: Parkinson's disease dementia

preAD: preclinical Alzheimer's disease

RBF: radial-basis function

ROC: receiver operating characteristic

SVM: support vector machine

UniPg: University of Perugia

UniPa: University of Palermo

XGBoost: eXtreme Gradient Boosting

Declarations

Acknowledgements and funding

This work was supported by Fondazione Perugia within the framework "Qualità della vita e sostenibilità del sistema sanitario: prevenzione, promozione della salute e potenziamento dell'assistenza territoriale" 2023 under Grant 21954 (2023.0524) and by the European Union - NextGenerationEU under the Italian Ministry of University and Research (MUR) National Innovation Ecosystem grant ECS00000041 - VITALITY - CUP J97G22000170005.

Competing Interests

G. Bellomo received honoraria from Fujirebio and completed paid consultancies for Parkinson's Foundation. He received travel/educational grants from Fujirebio and Alzheimer's Association. L. Parnetti served as Member of Advisory Boards for Fujirebio, IBL, Roche, and Merck. L. Gaetani has participated in advisory boards for and received writing or speaker honoraria and travel grants from Biogen, Eisai, Euroimmun, Fujirebio, Lilly, Novartis, Roche, and Siemens Healthineers. M. Ciaccio served as Member of Advisory Boards for Roche, Novartis and Lilly. L. Agnello served as Member of Advisory Boards for Novartis and Lilly. E.G. Torrigiani, D. Cianca, G. Nardi, I. Neri, L. Gammaitoni and D. Chiasserini have nothing to disclose.

Consent statement and ethics committee

All the procedures involving human subjects were performed following the Declaration of Helsinki. All participants gave written informed consent to use medical data and biomaterials for research purposes. The study was approved by the local Ethics Committees (UniPg: Comitato Etico Aziende Sanitarie Regione Umbria 19369/AV and 20942/21/OV, UniPa: Comitato Etico Palermo 1, verbale no. 02/2023).

Funding:

Fondazione Perugia; European Union - NextGenerationEU under the Italian Ministry of University and Research (MUR)

Author Contribution

E.G. Torrigiani and G. Bellomo conceived the article, gathered and analyzed data and drafted the manuscript;D. Cianca and I. Neri contributed to data analysis and interpretation;G. Nardi gathered data and performed biological measures on UniPg samples;L. Agnello and M. Ciaccio gathered data for UniPa and revised the manuscript;T. Piccoli gathered data for UniPa;D. Chiasserini, L.Parnetti and L. Gaetani contributed to data interpretation and revised all analyses and made major contributions to the drafting process;L. Gammaitoni revised data analysis and contributed to manuscript revision.

Acknowledgement

This work was supported by Fondazione Perugia within the framework "Qualità della vita e sostenibilità del sistema sanitario: prevenzione, promozione della salute e potenziamento dell'assistenza territoriale" 2023 under Grant 21954 (2023.0524) and by the European Union - NextGenerationEU under the Italian Ministry of University and Research (MUR) National Innovation Ecosystem grant ECS00000041 - VITALITY - CUP J97G22000170005.

Data Availability

The datasets used and/or analysed during the current study are available from the corresponding author on reasonable request.

References

1. Hansson O, Blennow K, Zetterberg H, Dage J. Blood biomarkers for Alzheimer's disease in clinical practice and trials. *Nat Aging*. 2023;3(5):506-519. doi:10.1038/s43587-023-00403-3
2. Janelidze S, Teunissen CE, Zetterberg H, et al. Head-to-Head Comparison of 8 Plasma Amyloid-β 42/40 Assays in Alzheimer Disease. *JAMA Neurol*. 2021;78(11):1375. doi:10.1001/jamaneurol.2021.3180
3. Olsson B, Lautner R, Andreasson U, et al. CSF and blood biomarkers for the diagnosis of Alzheimer's disease: a systematic review and meta-analysis. *Lancet Neurol*. 2016;15(7):673-684. doi:10.1016/S1474-4422(16)00070-3
4. Arranz J, Zhu N, Rubio-Guerra S, et al. Diagnostic performance of plasma pTau217, pTau181, Aβ1-42 and Aβ1-40 in the LUMIPULSE automated platform for the detection of Alzheimer disease. *Alzheimers Res Ther*. 2024;16(1):139.

doi:10.1186/s13195-024-01513-9

5. Bellomo G, Bayoumy S, Megaro A, et al. Fully automated measurement of plasma Aβ42/40 and p-tau181: Analytical robustness and concordance with cerebrospinal fluid profile along the Alzheimer's disease continuum in two independent cohorts. *Alzheimers Dement*. 2024;20(4):2453-2468. doi:10.1002/alz.13687
6. Janelidze S, Mattsson N, Palmqvist S, et al. Plasma P-tau181 in Alzheimer's disease: relationship to other biomarkers, differential diagnosis, neuropathology and longitudinal progression to Alzheimer's dementia. *Nat Med*. 2020;26(3):379-386. doi:10.1038/s41591-020-0755-1
7. Barthélemy NR, Horie K, Sato C, Bateman RJ. Blood plasma phosphorylated-tau isoforms track CNS change in Alzheimer's disease. *J Exp Med*. 2020;217(11):e20200861. doi:10.1084/jem.20200861
8. Mielke MM, Frank RD, Dage JL, et al. Comparison of Plasma Phosphorylated Tau Species With Amyloid and Tau Positron Emission Tomography, Neurodegeneration, Vascular Pathology, and Cognitive Outcomes. *JAMA Neurol*. 2021;78(9):1108. doi:10.1001/jamaneurol.2021.2293
9. Janelidze S, Berron D, Smith R, et al. Associations of Plasma Phospho-Tau217 Levels With Tau Positron Emission Tomography in Early Alzheimer Disease. *JAMA Neurol*. 2021;78(2):149. doi:10.1001/jamaneurol.2020.4201
10. Palmqvist S, Warmenhoven N, Anastasi F, et al. Plasma phospho-tau217 for Alzheimer's disease diagnosis in primary and secondary care using a fully automated platform. *Nat Med*. 2025;31(6):2036-2043. doi:10.1038/s41591-025-03622-w
11. Benedet AL, Brum WS, Hansson O, et al. The accuracy and robustness of plasma biomarker models for amyloid PET positivity. *Alzheimers Res Ther*. 2022;14(1):26. doi:10.1186/s13195-021-00942-0
12. Ashton NJ, Brum WS, Di Molfetta G, et al. Diagnostic Accuracy of a Plasma Phosphorylated Tau 217 Immunoassay for Alzheimer Disease Pathology. *JAMA Neurol*. 2024;81(3):255. doi:10.1001/jamaneurol.2023.5319
13. Jack CR, Andrews JS, Beach TG, et al. Revised criteria for diagnosis and staging of Alzheimer's disease: Alzheimer's Association Workgroup. *Alzheimers Dement*. 2024;20(8):5143-5169. doi:10.1002/alz.13859
14. U.S. Food and Drug Administration. FDA clears first blood test used in diagnosing Alzheimer's disease. Published online May 16, 2025. https://www.fda.gov/news-events/press-announcements/fda-clears-first-blood-test-used-diagnosing-alzheimers-diseas
15. Huang H, Liao Z, Wei X, Zhou Y. Combined Gaussian Mixture Model and Pathfinder Algorithm for Data Clustering. *Entropy*. 2023;25(6):946. doi:10.3390/e25060946
16. Bellomo G, Indaco A, Chiasserini D, et al. Machine Learning Driven Profiling of Cerebrospinal Fluid Core Biomarkers in Alzheimer's Disease and Other Neurological Disorders. *Front Neurosci*. 2021;15:647783. doi:10.3389/fnins.2021.647783
17. Magni E, Binetti G, Bianchetti A, Rozzini R, Trabucchi M. Mini-Mental State Examination: a normative study in Italian elderly population. *Eur J Neurol*. 1996;3(3):198-202. doi:10.1111/j.1468-1331.1996.tb00423.x
18. Dauphinot V, Calvi S, Moutet C, et al. Reliability of the assessment of the clinical dementia rating scale from the analysis of medical records in comparison with the reference method. *Alzheimers Res Ther*. 2024;16(1):198. doi:10.1186/s13195-024-01567-9
19. Jack CR, Bennett DA, Blennow K, et al. NIA-AA Research Framework: Toward a biological definition of Alzheimer's disease. *Alzheimers Dement*. 2018;14(4):535-562. doi:10.1016/j.jalz.2018.02.018
20. Postuma RB, Berg D, Stern M, et al. MDS clinical diagnostic criteria for Parkinson's disease: MDS-PD Clinical Diagnostic Criteria. *Mov Disord*. 2015;30(12):1591-1601. doi:10.1002/mds.26424
21. Emre M, Aarsland D, Brown R, et al. Clinical diagnostic criteria for dementia associated with Parkinson's disease. *Mov Disord*. 2007;22(12):1689-1707. doi:10.1002/mds.21507
22. Rascovsky K, Hodges JR, Knopman D, et al. Sensitivity of revised diagnostic criteria for the behavioural variant of frontotemporal dementia. *Brain*. 2011;134(9):2456-2477. doi:10.1093/brain/awr179
23. McKeith IG, Boeve BF, Dickson DW, et al. Diagnosis and management of dementia with Lewy bodies: Fourth consensus report of the DLB Consortium. *Neurology*. 2017;89(1):88-100. doi:10.1212/WNL.0000000000004058
24. Gorno-Tempini ML, Hillis AE, Weintraub S, et al. Classification of primary progressive aphasia and its variants. *Neurology*. 2011;76(11):1006-1014. doi:10.1212/WNL.0b013e31821103e6
25. Teunissen CE, Petzold A, Bennett JL, et al. A consensus protocol for the standardization of cerebrospinal fluid collection and biobanking. *Neurology*. 2009;73(22):1914-1922. doi:10.1212/WNL.0b013e3181c47cc2
26. Schwarz G. Estimating the Dimension of a Model. *Ann Stat*. 1978;6(2). doi:10.1214/aos/1176344136
27. Gaetani L, Chiasserini D, Paolini Paoletti F, Bellomo G, Parnetti L. Required improvements for cerebrospinal fluid-based biomarker tests of Alzheimer's disease. *Expert Rev Mol Diagn*. 2023;23(12):1195-1207. doi:10.1080/14737159.2023.2276918

28. Schindler SE, Galasko D, Pereira AC, et al. Acceptable performance of blood biomarker tests of amyloid pathology — recommendations from the Global CEO Initiative on Alzheimer's Disease. *Nat Rev Neurol*. 2024;20(7):426-439. doi:10.1038/s41582-024-00977-5
29. Maltarollo VG, Kronenberger T, Espinoza GZ, Oliveira PR, Honorio KM. Advances with support vector machines for novel drug discovery. *Expert Opin Drug Discov*. 2019;14(1):23-33. doi:10.1080/17460441.2019.1549033
30. Chen T, Guestrin C. XGBoost: A Scalable Tree Boosting System. In: *Proceedings of the 22nd ACM SIGKDD International Conference on Knowledge Discovery and Data Mining*. ACM; 2016:785-794. doi:10.1145/2939672.2939785
31. Li W, Peng Y, Peng K. Diabetes prediction model based on GA-XGBoost and stacking ensemble algorithm. Rathnayake U, ed. *PLOS ONE*. 2024;19(9):e0311222. doi:10.1371/journal.pone.0311222
32. Hunter JD. Matplotlib: A 2D Graphics Environment. *Comput Sci Eng*. 2007;9(3):90-95. doi:10.1109/MCSE.2007.55
33. Virtanen P, Gommers R, Oliphant TE, et al. SciPy 1.0: fundamental algorithms for scientific computing in Python. *Nat Methods*. 2020;17(3):261-272. doi:10.1038/s41592-019-0686-2
34. Waskom M. seaborn: statistical data visualization. *J Open Source Softw*. 2021;6(60):3021. doi:10.21105/joss.03021
35. Harris CR, Millman KJ, Van Der Walt SJ, et al. Array programming with NumPy. *Nature*. 2020;585(7825):357-362. doi:10.1038/s41586-020-2649-2
36. McKinney W. Data Structures for Statistical Computing in Python. In: 2010:56-61. doi:10.25080/Majora-92bf1922-00a
37. Pedregosa F, Varoquaux G, Gramfort A, et al. Scikit-learn: Machine Learning in Python. Published online 2012. doi:10.48550/ARXIV.1201.0490
38. Terpilowski M. scikit-posthocs: Pairwise multiple comparison tests in Python. *J Open Source Softw*. 2019;4(36):1169. doi:10.21105/joss.01169
39. Scrucca L, Fraley C, Murphy TB, Adrian E. R. *Model-Based Clustering, Classification, and Density Estimation Using Mclust in R*. 1st ed. Chapman and Hall/CRC; 2023. doi:10.1201/9781003277965
40. Gillespie NA, Elman JA, McKenzie RE, et al. The heritability of blood-based biomarkers related to risk of Alzheimer's disease in a population-based sample of early old-age men. *Alzheimers Dement*. 2024;20(1):356-365. doi:10.1002/alz.13407

Tables

Table 1. Distribution of plasma biomarkers values across diagnostic groups in a) UniPg cohort and b) UniPa cohort. All values are expressed as mean +/- standard deviation. (n): number of patients for which plasma pTau217 was available; preAD: preclinical Alzheimer's Disease; AD-MCI: Mild Cognitive Impairment due to Alzheimer's Disease; ADdem: dementia due to Alzheimer's Disease; PD-CN: cognitively unimpaired Parkinson's Disease; PD-MCI: Parkinson's Disease with Mild Cognitive Impairment; PDD/DLB: Parkinson's Disease Dementia/Dementia with Lewy Bodies; FTD: Fronto-Temporal Dementia; OND: Other Neurological Disease; CTRL: subjects without specific pathological phenotypes and with a non-AD CSF profile; A+: % of patients with CSF with an A+ CSF profile; T+: % of patients with CSF with a T+ CSF profile.

a) Groups	N (N pTau217)	Sex (M/F)	Age (years)	Education (years)	MMSE	A+ (%)	T+ (%)	Plasma Aβ42/40	Plasma pTau181 (pg/mL)	Plasma pTau217 (pg/mL)
preAD	30 (24)	13/17	72.3 ± 5.1	10.0 ± 4.3	28.0 ± 1.4	100%	100%	0.076 ± 0.015	1.9 ± 1.0	0.262 ± 0.163
AD-MCI	141 (127)	44/97	72.9± 6	10.1 ± 4.7	23.9 ± 3.1	100%	100%	0.076 ± 0.011	2.8 ± 1.4	0.627 ± 0.353
ADdem	114 (95)	29/75	73.5± 6.7	8.8 ± 4.5	15.5 ± 6.1	100%	100%	0.078 ± 0.009	3.3 ± 1.1	0.902 ± 0.515
PD-CN	40 (36)	23/17	65.9 ± 6.2	11.8 ± 4.1	28.4 ± 1.5	7%	18%	0.095 ± 0.029	1.1 ± 0.6	0.072 ± 0.038
PD-MCI	55 (43)	40/15	69.3 ± 6.5	9.7 ± 3.7	26.0 ± 2.0	24%	21%	0.092 ± 0.020	1.4 ± 0.7	0.12 ± 0.086
PDD/DLB	17 (11)	16/1	72.5 ± 10.5	8.6 ± 4.4	20.6 ± 5.2	67%	50%	0.077 ± 0.013	2.3 ± 1.0	0.43 ± 0.348
FTD	32 (18)	18/14	72.2 ± 6.7	9.4 ± 3.9	23.2 ± 3.8	24%	27%	0.083 ± 0.012	2.0 ± 0.7	0.30 ± 0.31
OND	32 (32)	16/16	72.9 ± 7.1	10.0 ± 4.5	22.7 ± 5.4	56%	26%	0.082 ± 0.023	2.0 ± 0.9	0.219 ± 0.146
CTRL	140 (104)	81/59	69.5 ± 7.1	10.3 ± 4.5	26.7 ± 2.16	0%	18%	0.084 ± 0.016	1.7 ± 1.4	0.149 ± 0.177

b) Groups	N	Sex (M/F)	Age (years)	Education (years)	MMSE	A+ (%)	T+ (%)	Plasma pTau217 (pg/mL)
AD-MCI	39	19/20	71.4± 6.86	10.1 ± 4.9	23.7 ± 4.2	100%	100%	0.590 ± 0.330
ADdem	55	26/29	69.9± 7.6	9.5 ± 4.3	18 ± 6.3	100%	95%	0.722 ± 0.344
PDD/DLB	2	0/2	77 ± 5.7	17 ± 0	15.5 ± 13.4	100%	0%	0.333 ± 0.011
OND	7	4/3	73.5 ± 4.3	8.1 ± 4.3	15.1 ± 9.8	71%	14%	0.312 ± 0.188
CTRL	14	5/9	68.9 ± 7.6	10.7 ± 4.4	25.9 ± 3.1	35%	0%	0.174 ± 0.084

Figures

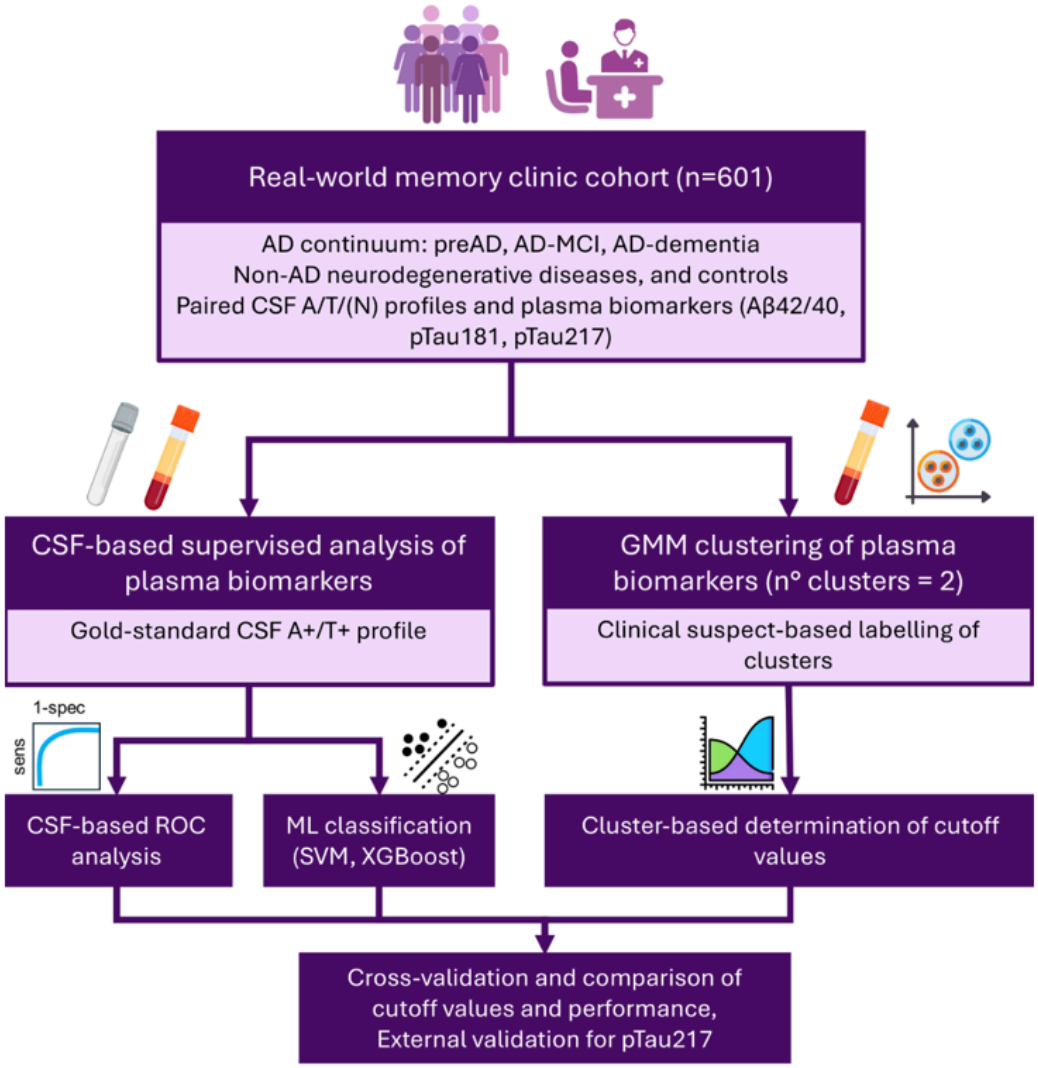


Figure 1

Study design and analytical workflow. A real-world memory-clinic cohort (n = 601) with paired plasma and CSF biomarkers was analyzed through parallel supervised and unsupervised machine-learning pipelines. In the supervised arm, CSF-referenced ROC and ML classifiers (SVM, XGBoost) were applied to plasma Aβ42/40, pTau181, and pTau217 (available for n=490). In the unsupervised arm, GMM clustering of plasma biomarkers generated CSF-independent, data-driven cutoffs. Cutoff values and diagnostic performances generated via supervised and unsupervised approaches were then compared and for pTau 217 tested in an independent validation cohort from UniPa.

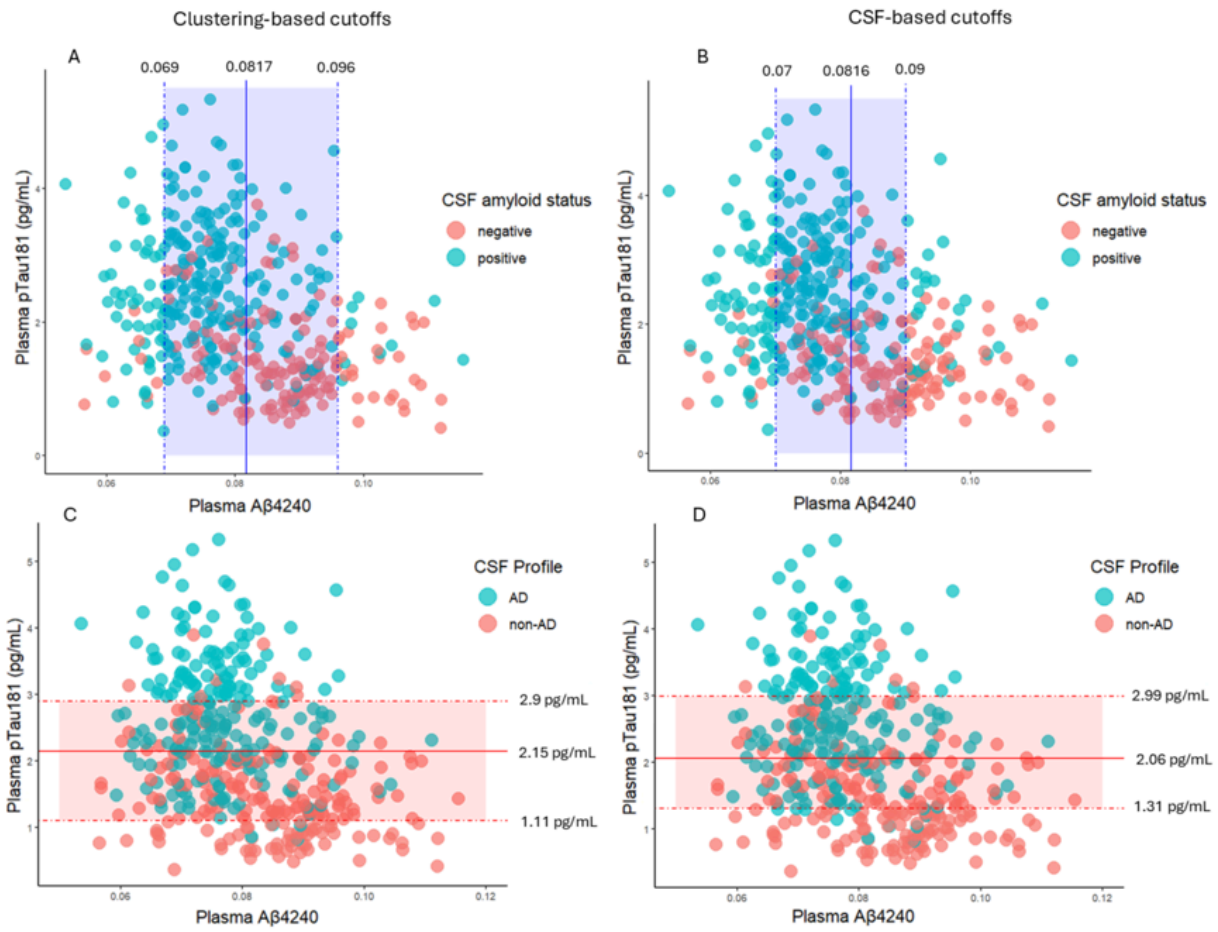


Figure 2

Plasma Aβ42/40 and pTau181 distributions and cutoff values.

A, clustering-based cutoff values for plasma Aβ42/40 (solid line: 50% cluster 1 cutoff, dotted lines: 95% cluster 1 and 5% cluster 1 cutoffs, colored area: patients falling between 95% and 5 % cluster 1 cutoffs); B, CSF-based cutoff values for plasma Aβ42/40 (solid line max YI cutoff, dotted lines 95%sens and 95%spec cutoffs, colored area patients falling between 95%sens and 95% spec cutoffs); C, clustering-based cutoff values for plasma pTau181 (solid line: 50% cluster 1 cutoff, dotted lines: 95% cluster 1 and 5% cluster 1 cutoffs, colored area: patients falling between 95% and 5 % cluster 1 cutoffs); D, CSF-based cutoff values for plasma pTau181 (solid line max YI cutoff, dotted lines 95%sens and 95%spec cutoffs, colored area patients falling between 95%sens and 95% spec cutoffs)

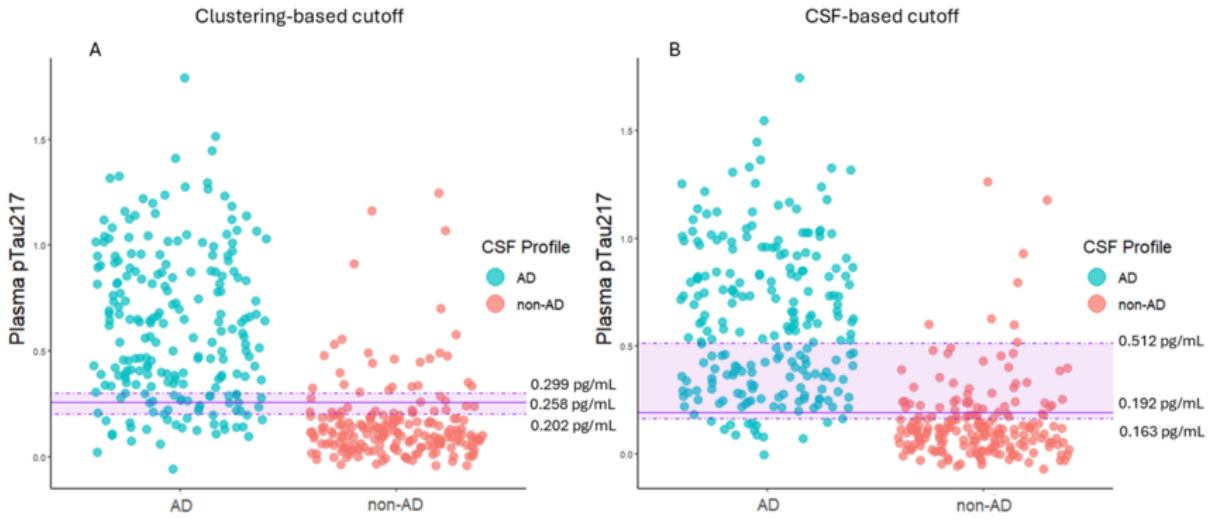


Figure 3

plasma pTau217 distribution and cutoff values in UniPg cohort. A, clustering-based cutoff values for plasma pTau217 (solid line: 50% cluster 1 cutoff, dotted lines: 95% cluster 1 and 5% cluster 1 cutoffs, colored area: patients falling between 95% and 5 % cluster 1 cutoff); B, CSF-based cutoff values for plasma pTau217 (solid line: max YI cutoff, dotted lines: 95%sens and 95%spec cutoffs, colored area: patients falling between 95%sens and 95% spec cutoffs)

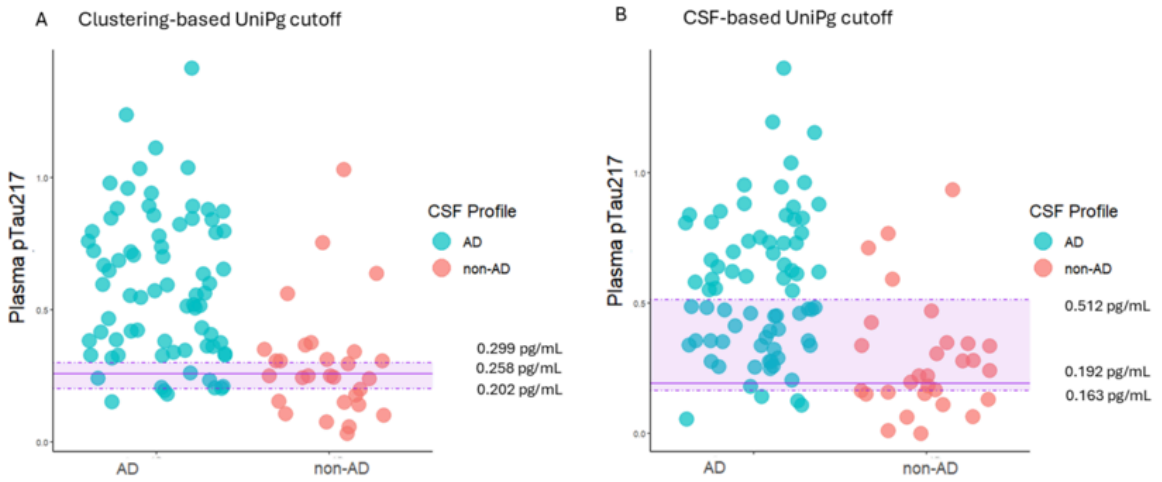


Figure 4

plasma pTau217 distribution and cutoff values in UniPa cohort. A, clustering-based cutoff values for plasma pTau217 generated in UniPg cohort (solid line: 50% cluster 1 cutoff, dotted lines: 95% cluster 1 and 5% cluster 1 cutoffs, colored area: patients falling between 95% and 5 % cluster 1 cutoff); B, CSF-based cutoff values for plasma pTau217 generated in UniPg cohort (solid line: max YI cutoff, dotted lines: 95%sens and 95%spec cutoffs, colored area: patients falling between 95%sens and 95% spec cutoffs).

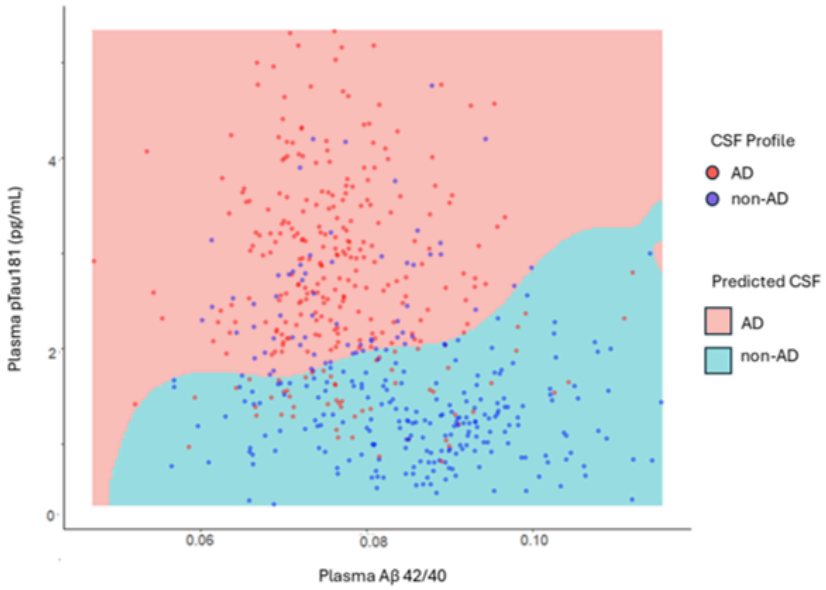


Figure 5

Graphic representation of SVM supervised classifier based upon plasma Aβ42/40 and plasma pTau181.

Colored areas: region of BBM distribution with SVM-predicted AD CSF, in pale red, region of BBM distribution with SVM-predicted non-AD CSF, in light blue; dots: subjects with defined CSF AD profile, red dots, subjects with defined CSF non-AD profile, blue dots.

Supplementary Files

This is a list of supplementary files associated with this preprint. Click to download.

- SupplementaryMaterial.docx